J|A|C|S
COMMUNICATIONS

Published on Web 07/11/2008

Electronic Properties of Conjugated Polyelectrolyte Thin Films

Jung Hwa Seo and Thuc-Quyen Nguyen*

Department of Chemistry and Biochemistry, Center for Polymers and Organic Solids, University of California, Santa Barbara, California 93106

Received March 3, 2008; E-mail: quyen@chem.ucsb.edu

Conjugated polyelectrolytes (CPEs) contain a π-delocalized backbone with pendant groups capable of ionizing in high dielectric media. Their solubility in polar solvents allows fabrication of multilayer polymer-based light emitting diodes (PLEDs) in combination with neutral conjugated polymers by taking advantage of solvents with orthogonal polarities.[1] CPEs have been used as electron injection layers in PLEDs. The function of PLEDs depends strongly on the interface of polymer/metal electrodes.[2–4] The exact electronic structure of the polymer/metal interface is therefore an important consideration from both a fundamental science perspective and for being able to better design materials for incorporation into optoelectronic devices.[5–7]

Cyclic voltammetry (CV) studies have been carried out on CPEs and have shown no difference in the energy levels for a given backbone, whether the pendant groups are charged or not[8] (Supporting Information). However, this information is obtained in contact with solution and in the presence of an electrolyte.[9] The situation in neat films is thus expected to be different. Ultraviolet photoelectron spectroscopy (UPS) is a well-established analytical technique for obtaining the energy levels in organic thin films.[6] When ultraviolet photons are incident on the sample, valence electrons are ejected to the vacuum. The kinetic energies of the escaping electrons are measured and are used to obtain information such as the highest occupied molecular orbital (HOMO) level, work function, electron affinity (E_A), ionization potential (I_P), and interfacial dipoles.[7] Herein we provide a study of the energy levels of a representative CPE structure as a function of whether the backbone contains neutral, anionic, or cationic pendant groups. We also probe the effect of the charge compensating counterions in the case of the cationic structure.

Scheme 1 shows the polymer structures used in this study. The materials are as follows: (a) poly[9,9-bis[6′-(*N*,*N*,*N*-trimethylammonium)hexyl]fluorene-*alt*-*co*-1,4-phenylene]bromide (**PFN$^+$Br$^-$**), (b) poly[9,9-bis[6′-(*N*,*N*,*N*-trimethylammonium)hexyl]fluorene-*alt*-*co*-1,4-phenylene]tetrakis(imidazoly)borate (**PFN$^+$BIm$_4^-$**), (c) the neutral precursor of **PFN$^+$Br$^-$** (**PFN-Br**), and (d) sodium poly[9,9-bis(4′-sulfonatobutyl)fluorine-*alt*-*co*-1,4-phenylene] (**PFNSO$_3^-$Na$^+$**). Films were deposited by spin-coating from 0.2% (w/v) solutions in different solvents (chlorobenzene for **PFN-Br**, methanol for **PFN$^+$Br$^-$**, and **PFN$^+$BIm$_4^-$** and a 2:1 mixture of methanol and water for **PFNSO$_3^-$Na$^+$**). UV−vis absorption spectra were collected from films spin-coated onto quartz substrates. For UPS measurements, the polymers were spin-coated atop a 100 nm thick Au layer that was deposited onto a SiO_2/Si substrate. The thicknesses of the CPEs were determined to be ∼5 nm for **PFN-Br**, **PFN$^+$Br$^-$**, and **PFNSO$_3^-$Na$^+$**, and ∼3 nm for **PFN$^+$BIm$_4^-$** by atomic force microscopy (AFM) measurements (Supporting Information). Films were fabricated inside a N_2 atmosphere globebox and were transferred via an airtight sample holder to the UPS analysis chamber. Samples were subsequently kept in a high-vacuum chamber overnight to remove solvent residues. The UPS analysis chamber was equipped with a hemispherical electron energy analyzer (Kratos Ultra Spectrometer) and a UV (He I) source and was maintained at 1×10^{-9} Torr. UPS spectra were collected along a direction normal to the surface with a photon incidence angle of 35°. A sample bias of −9 V was used to acquire the high binding energy cutoff.[10] All measurements were made in triplicate.

Scheme 1. Chemical Structures of (a) **PFN$^+$Br$^-$**, (b) **PFN$^+$BIm$_4^-$**, (c) **PFN-Br**, and (d) **PFNSO$_3^-$Na$^+$**

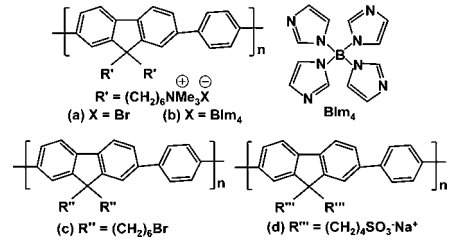

Table 1. Summary of Results from UV−Vis and UPS Measurements (eV)

	E_g	ϕ_{hole}	$\phi_{electron}$	I_P	E_A	Δ
PFN-Br	2.98	1.22	1.76	6.36	3.38	+0.19
PFN$^+$Br$^-$	2.95	1.68	1.27	6.07	3.12	−0.56
PFN$^+$BIm$_4^-$	2.96	1.75	1.21	6.17	3.21	−0.53
PFNSO$_3^-$Na$^+$	2.95	1.15	1.80	6.15	3.20	+0.05

Absorption spectra were employed to determine the optical energy band gap (E_g). Although optical E_g is smaller than the true E_g because it does not take into account the exciton binding energy, it can be generally used to estimate HOMO−LUMO energy difference.[7,10] The absorption onset was determined by linear extrapolation of the low energy edge of the spectrum (Supporting Information). As expected, the E_g values for the CPE materials with different counterion and charge are similar since they have the same conjugated backbone and are slightly larger than that for the neutral **PFN-Br**(Table 1).

Figure 1 shows the UPS results for the different CPE films and a Au layer to reference the Fermi energy level (E_F). The abscissa is the binding energy relative to the E_F of Au, which is defined by the energy of the electron before excitation relative to the vacuum level (E_{vac}). The polymer HOMO energy levels were calculated using the low binding energy region (0−4 eV). Here the spectra have been extended in the intensity direction to identify the lowest energy level. The HOMO onsets of **PFN-Br**, **PFN$^+$Br$^-$**, **PFN$^+$BIm$_4^-$**, and **PFNSO$_3^-$Na$^+$** are 1.22, 1.68, 1.75 and 1.15 eV, respectively.

Examination of the high binding energy cutoff (E_{cutoff}) region in Figure 1 (12−18 eV) allows one to extract the shift in the E_{vac}. Deposition of **PFN$^+$Br$^-$** and **PFN$^+$BIm$_4^-$** leads to a shift toward higher energies, while for the neutral and anionic polymer, the changes are less pronounced. The shift of E_{vac} indicates the magnitude of the interfacial dipole (Δ), which is equal to subtracting the work function of Au (ϕ_{Au}) from the difference between the E_{vac}

10.1021/ja801451e CCC: $40.75

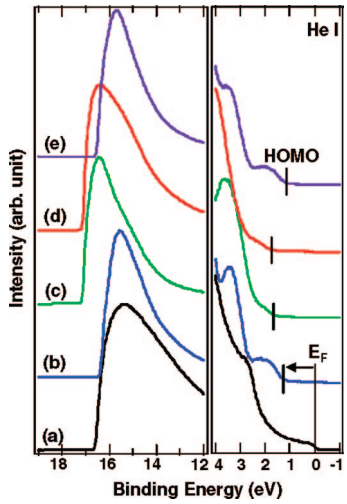

Figure 1. UPS spectra of (a) Au reference, (b) **PFN-Br**, (c) **PFN$^+$Br$^-$**, (d) **PFN$^+$BIm$_4^-$**, and (e) **PFNSO$_3^-$Na$^+$**. LHS: High binding energy cutoff region. The intensity is normalized relative to the maximum point. RHS: HOMO region. The intensities are magnified along the ordinate to highlight spectral comparison.

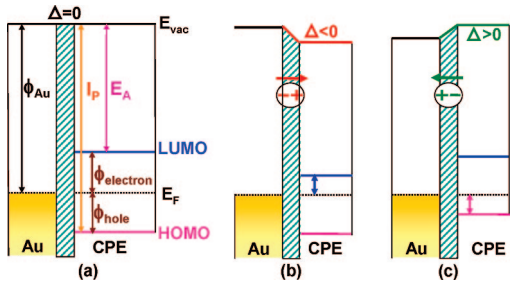

Figure 2. Energy diagrams near the Au/conjugated polyelectrolyte interface (a) in the vacuum level alignment and in the presence of an interfacial dipole with (b) negative and (c) positive magnitude.

of the CPE layer and E_F. The I_P is also determined by using the incident photon energy (21.2 eV), the E_{cutoff}, and the onset of the HOMO according to the equation[5]

$$I_P = 21.2 - (E_{cutoff} - \text{HOMO}) \quad (1)$$

The LUMO level is estimated by using the HOMO and E_g values, while the E_A is derived by using E_{vac} and the LUMO level.[11] Table 1 contains a summary of these variables.

The difference between the HOMO and E_F as shown in Figure 2a would correspond to the hole injection barrier (ϕ_{hole}) in optoelectronic devices.[12] The value between E_F and the LUMO level is also frequently used as a measure of the electron injection barrier ($\phi_{electron}$). One observes from Table 1 that $\phi_{hole} > \phi_{electron}$ by 0.41 and 0.54 eV for **PFN$^+$Br$^-$** and **PFN$^+$BIm$_4^-$**, respectively, while $\phi_{hole} < \phi_{electron}$ by 0.54 and 0.65 eV for **PFN-Br** and **PFNSO$_3^-$Na$^+$**, respectively. Thus, despite the fact that all polymers have identical backbone, one would expect that, at least with a Au electrode, electron injection would be expected to be more facile for **PFN$^+$Br$^-$** and **PFN$^+$BIm$_4^-$**, while hole injection would be preferred for **PFN-Br** and **PFNSO$_3^-$Na$^+$**. This result is consistent with a significant lower electron current density observed in electron-only diodes fabricated from **PFNSO$_3^-$Na$^+$** than from **PFN$^+$Br$^-$**.[2b]

One possible explanation for lowering electron barriers in **PFN$^+$Br$^-$** and **PFN$^+$BIm$_4^-$** is the formation of an interfacial dipole with the positive pole pointing toward the polymer layer and the negative pole toward the metal (Figure 2b).[13] Conversely, positive interfacial dipole is directed toward the metal surface upon deposition of **PFN-Br**, thereby raising the E_{vac} outside the electrode, as shown in Figure 2c.[13] For **PFNSO$_3^-$Na$^+$**, there is only a negligible dipole effect. Therefore, on the basis of our analysis of absorption and UPS measurements, and in contrast to expectations raised by CV measurements, there are substantial differences in the electronic properties of CPEs deposited atop a Au surface as a function of charge and counterion. The exact magnitude of the injection barriers is likely a result of an interplay between the intrinsic electronic structure of the polymers and the net alignment of dipoles at the metal/organic interface, the self-assembly of which remains poorly understood.

In conclusion, we have examined four conjugated polymers with identical backbone but with different pendant charges and charge compensating ions for the case of the cationic structures. The results of absorption and UPS measurement show different molecular orbital energy levels, I_P, and E_A. These studies highlight the need for better characterization of polymer organization adjacent to the metal and reveal that substantially different properties can be achieved for a given polymer structure by variations of functional groups that are removed from the semiconducting, electronically delocalized framework.

Acknowledgment. The authors thank the NSF CAREER grant (DMR# 0547639) for the financial support. We thank Jacek Z. Brzezinski, Renqiang Yang, Bright Walker, and Guillermo C. Bazan for the materials, and Mananya Tantiwiwat for assistance with the gold surface preparation.

Supporting Information Available: UV–vis absorption spectra, CV data, and AFM images of each CPE are available. This material is available free of charge via the Internet at http://pubs.acs.org.

References

(1) (a) Yang, R.; Wu, H.; Cao, Y.; Bazan, G. C. *J. Am. Chem. Soc.* **2006**, *128*, 14422–14423. (b) Huang, F.; Wang, X.; Wang, D.; Yang, W.; Cao, Y. *Polymer* **2005**, *46*, 12010–12011.
(2) (a) Hoven, C.; Yang, R.; Garcia, A.; Heeger, A. J.; Nguyen, T.-Q.; Bazan, G. C. *J. Am. Chem. Soc.* **2007**, *129*, 10976–10977. (b) Garcia, A.; Yang, R.; Jin, Y.; Walker, B.; Nguyen, T.-Q. *Appl. Phys. Lett.* **2007**, *91*, 153502.
(3) Gong, X.; Wang, S.; Moses, D.; Bazan, G. C.; Heeger, A. J. *Adv. Mater.* **2005**, *17*, 2053–2058.
(4) Ma, W. L.; Iyer, P. K.; Gong, X.; Liu, B.; Moses, D.; Bazan, G. C.; Heeger, A. J. *Adv. Mater.* **2005**, *17*, 274–277.
(5) (a) Salaneck, W. R.; Lögdlund, M.; Fahlman, M.; Greczynski, G.; Kugler, Th. *Mater. Sci. Eng. R* **2001**, *34*, 121–146. (b) Liao, L. S.; Fung, M. K.; Lee, C. S.; Lee, S. T.; Inbasekaran, M.; Woo, E. P.; Wu, W. W. *Appl. Phys. Lett.* **2000**, *76*, 3582–3584.
(6) (a) Koch, N.; Kahn, A.; Ghijsen, J.; Pireaux, J.-J.; Schwarz, J.; Johnson, R. L.; Elschner, A. *Appl. Phys. Lett.* **2003**, *82*, 70–72. (b) Bruner, E.; Koch, N.; Span, A. R.; Bernasek, S. L.; Kahn, A.; Schwartz, J. *J. Am. Chem. Soc.* **2002**, *124*, 3192–3193. (c) Watkins, N. J.; Mäkinen, A. J.; Gao, Y.; Uchida, M.; Kafafi, Z. H. *J. Appl. Phys.* **2006**, *100*, 103706.
(7) (a) Ishii, H.; Sugiyama, K.; Ito, E.; Seki, K. *Adv. Mater.* **1999**, *11*, 605–625. (b) Tengstedt, C.; Osikowicz, W.; Salaneck, W. R.; Parker, I. D.; Hsu, C.-H.; Fahlman, M. *Appl. Phys. Lett.* **2006**, *88*, 053502.
(8) (a) Huang, F.; Hou, L. T.; Wu, H. B.; Wang, X. H.; Shen, H. L.; Cao, W.; Yang, W.; Cao, Y. *J. Am. Chem. Soc.* **2004**, *126*, 9845. (b) Zhang, Y.; Xu, Y. H.; Niu, Q. L.; Peng, J. B.; Yang, W.; Zhu, X. H.; Cao, Y. *J. Mater. Chem.* **2007**, *17*, 992.
(9) (a) Hsieh, B. Y.; Chen, Y. *Macromolecules* **2007**, *40*, 8913–8923. (b) Chaur, M. N.; Melin, F.; Elliott, B.; Athans, A. J.; Walker, K.; Holloway, B. C.; Echegoyen, L. *J. Am. Chem. Soc.* **2007**, *129*, 14826–14829. (c) Juliard, A. L.; Shalit, H. *J. Electrochem. Soc.* **1963**, *110*, 1002–1006.
(10) Seo, J. H.; Pedersen, T. M.; Chang, G. S.; Moewes, A.; Yoo, K.-H.; Cho, S. J.; Whang, C. N. *J. Phys. Chem. B* **2007**, *111*, 9513–9518.
(11) (a) Chang, C.-H.; Liao, J.-L.; Hung, M.-C.; Chen, S.-A. *Appl. Phys. Lett.* **2007**, *90*, 063506. (b) Dam, N.; Beerbom, M. M.; Braunagel, J. C.; Schlaf, R. *J. Appl. Phys.* **2005**, *97*, 024909.
(12) Parker, I. D. *J. Appl. Phys.* **1994**, *75*, 1665.
(13) (a) Khodabakhsh, S.; Poplavskyy, D.; Heutz, S.; Nelson, J.; Bradley, D. D. C.; Murata, H.; Jones, T. S. *Adv. Funct. Mater.* **2004**, *14*, 1205–1210. (b) Crispin, X.; Geskin, V.; Crispin, A.; Cornil, J.; Lazzaroni, R.; Salaneck, W. R.; Bresdas, J.-L. *J. Am. Chem. Soc.* **2002**, *124*, 8131–8141.

JA801451E